Differences of radiological artefacts in cochlear implantation in temporal bone and complete head

Isabell Diogo, Nora Franke, Silke Steinbach-Hundt, Magis Mandapathil, Rainer Weiss, J. A. Werner, Christian Güldner

Department of ENT, Head and Neck surgery, University of Marburg, UKGM, Germany

Objectives: Accurate radiological evaluation of cochlear implants is essential for improvement of devices and techniques and also for assessing the position of the electrodes within the cochlea. Radiological study of implants has focused on isolated temporal bones. Previous studies showed relevant sizes of artefacts (dimensions of the radiological image compared with the actual dimensions of the electrode) in visualization of cochlear implants in computed tomography and cone beam computed tomography (CBCT). In this study, we aimed to obtain CBCT images of cochlear electrodes in isolated temporal bones and in whole heads and to assess the differences in image quality between the two.

Methods: Cochlear electrodes were implanted in three complete human heads. Radiological examinations were performed using a single CBCT scanner with varying x-ray tube currents, voltages, and rotation angles. The temporal bones were then removed and the same radiological examinations were repeated, with and without the receiver coils. Artefacts from a basal electrode (electrode 9) and an apical electrode (electrode 2) were calculated. These were compared with each other by measuring the diameter of the image of the electrode (electrode inclusive of imaging artefacts) and with the real electrode diameters from the manufacturer's data. Additionally, the radiological diameters (inclusive of artefact) of the electrodes were compared to the cross-sectional diameters of the basal and apical coils of the cochlea at the locations of these two electrodes.

Results: In comparison to the real electrode diameters, radiological artefact proportions of 51–58% for electrode 9 and 56–61% for electrode 2 were calculated. The differences between whole head images (group 1) and temporal bone images with and without the receiver coil (groups 2 and 3) were highly significant for each protocol ($P < 0.001$).

Discussion and conclusion: These results indicate that it is not possible reliably to determine the exact intracochlear positions of electrodes using CBCT. Imaging of isolated temporal bones produced significantly greater artefacts than imaging of the whole head. Evaluations of image quality based only on results for isolated temporal bones are not transferable to clinical situations, and should be assessed critically.

Keywords: Cochlear implantation, Artefacts, Cone beam computed tomography, Digital volume tomography, Temporal bone, Flex soft electrode

Introduction

Cochlear implantation has become an important treatment of congenital or acquired sensorineural hearing loss. Alongside the technical advances of the devices themselves, there has been a mounting discussion about the different operating procedures and their audiological results. One aspect of comparison of operating strategies is the determination of the exact intracochlear position of the electrodes. Today, high resolution computed tomography (CT) and cone beam CT (CBCT) are available for intra- and post-operative imaging, and in particular, CBCT has gained more interest because it offers higher resolution and lower radiation exposure in comparison to standard CT (Kolditz *et al.*, 2011; Dalchow *et al.*, 2006a). A further advantage of CBCT is that due to its physical protocols, a lower rate of metal artefacts is expected, which is most important in visualizing small structures (Dalchow *et al.*, 2006b). The term metal artefacts refer to the fact that the apparent dimensions of the metal electrodes on the CT images are larger that the actual dimensions of these electrodes.

Correspondence to: Dr. Christian Gueldner, Department of ENT, Head and Neck Surgery, University Hospital of Marburg, Baldingerstraße, Marburg 35043, Germany. Email: gueldner@staff.uni-marburg.de

DOI 10.1179/1754762813Y.0000000035

Until now, because of practicality, *in vitro* studies on cochlear implants have been performed nearly exclusively on isolated temporal bones, and whether or not it is possible to transfer these results into real clinical situations with the whole head has not been thoroughly evaluated. In a previous study, proportions of radiological artefacts of intracochlear electrodes of about 50% (i.e. the radiological images were 50% greater than the real electrode size) were determined in visualization of cochlear electrodes in whole human heads by CBCT (Güldner *et al*., 2011b).

Based on that study, the aim of this study was to determine differences of radiological artefact proportions between CBCT images of the whole head and of the corresponding isolated temporal bone and to look at the role of temporal bone models in imaging research. The second aim was to analyse the proportions of the radiological artefacts in CBCT images of cochlear electrodes at two different positions in the cochlea and to look for potential limitations in postoperative imaging of implants.

Methods

Three complete human heads (including soft tissue and brain structures) were obtained for radiological and surgical analysis. Heads were from human donors who dedicated their bodies for human research. To create a simulation of *in vivo* human cochlear implantation, complete implants (electrode with cable and coil) were used. After sub-total mastoidectomy and posterior tympanotomy, the round window was exposed. To visualize the entire round window, the bony overhang was drilled down, while protecting of the round window membrane. Afterwards, full cochlear insertion of the flex soft electrode (MedEl, 31 mm) was performed. A bed was drilled for the implant and the implant was fixed by multiple sutures.

After implantation, radiological examinations were performed using a single CBCT machine (Accu-I-tomo F17, Morita, Kyoto, Japan) with the head positioned in the normal position on the moveable stand. Seventy examinations varying the angle of rotation, the x-ray tube current, and the x-ray tube voltage were performed for each head. The rotation angle varied between 360 (exposure time, 17 seconds) and 180° (exposure time, 9 seconds). An advantage of the 180° mode is lower irradiation of the lenses of the eyes because of backwards rotation of the head. The tube current varied between 2 and 10 mA (2, 4, 6, 8, and 10 mA) and the tube voltage between 72 and 90 kV (72, 76, 80, 84, 86, 88, and 90 kV). The region of interest was defined according to standard procedures in imaging of the temporal bone by a cylinder with a diameter and height of 6 cm.

Next, the cable between the intracochlear electrode and the rest of the implant was cut, and the electrode was fixed in the round window niche. Afterwards, with the assistance of our colleagues of the Department of Pathology, the implanted temporal bones were extracted and the same radiological examinations described above were performed on the isolated temporal bones. These examinations were performed with and then without the implant receiver coil, so that altogether, there were three groups of images for analysis: group 1, whole head with electrode and implant receiver coil; group 2, temporal bone with electrode and implant receiver coil; and group 3, temporal bone with electrode alone (without receiver coil).

All further measurements were performed by the first author with a special graphic program (Photoshop CS2; Miami, FL, USA). The complete radiological diameter of the electrodes (inclusive of the metal artefacts) was measured at the basal part (electrode 9) and at the apical part of the electrode array (electrode 2). In the MedEl Flex implant, the five most apical electrodes (including electrode 2) have a single electrode terminal, or 'plate' on the surface of the silicone electrode array, while the remaining seven more basal electrodes each have two 'plates' on either aspect of the silicone array (Fig. 1). Because of the asymmetry between the views of the electrodes when viewed from the side and from above, the diameter was evaluated in all three dimensions (coronal, axial, sagittal) of the image (Fig. 2) and a mean diameter was calculated. In the case of the seven basal electrodes, including electrode 9, the two terminal plates produced a single image. The goal of these measurements was to compare the radiological images of the electrodes with their true diameters (according to data provided by MedEl) to determine the radiological artefact, as a percentage by which the image was larger than the true electrode size. Additionally, at the positions of electrodes 2 and 9 within the cochlea the cross-sectional diameter of the cochlear coil at that point was measured (Fig. 2C). To look for possible errors in this kind of measurement, the radiographic measurements of the electrode cable (cable with silicone sheath) were compared with the real electrode dimensions published in the manufacturer's data and the proportion of the image represented by the artefact calculated as a percentage.

To analyse the extent of artefact in CBCT visualization of the electrodes, measurements based on CBCT were compared with the actual diameters of the electrodes provided in the data sheets of the MedEl company. Statistical analyses (*t*-test, significance level $P < 0.01$) were performed with SPSS 17.0 (SPSS Inc., Chicago, IL, USA).

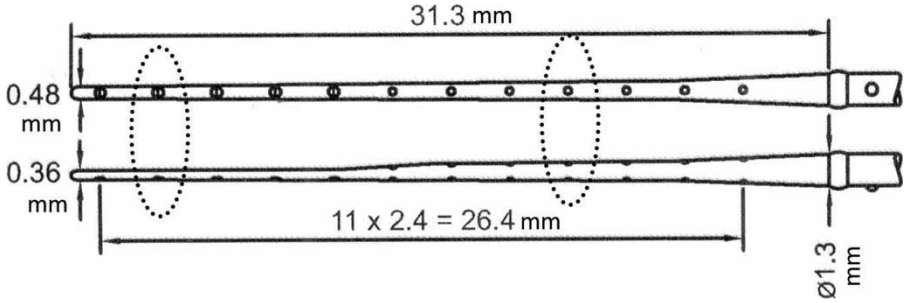

Figure 1 Technical views of the electrodes and the relevant diameters from above (upper diagram) and lateral view (lower diagram) according to the modified data sheet of MedEl. The asymmetry of the tip of the electrode can be seen easily.

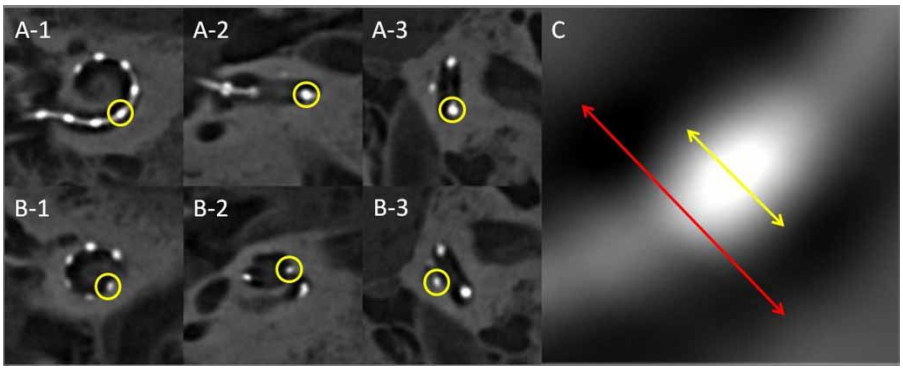

Figure 2 View of electrode 9 in the basal part of the cochlea (A) and electrode 2 in the apical part of the cochlea (B) in coronal (1), axial (2), and sagittal (3) slices. (C) illustrates the measurement of the radiological diameter of the image of the electrode (yellow arrow) and the corresponding diameter of the cross-section of the turn of the cochlea (red arrow).

Results

The surgical procedure was possible in all three heads. The position of the electrodes after extracting the temporal bones was confirmed by macroscopic and microscopic evaluation and all radiological examinations were performed without problems. Despite the differences of imaging quality, because of the variation of the x-ray tube settings, a reliable evaluation of the electrodes was possible (Fig. 3).

The published diameters of the electrodes from the manufacturer data sheets were 0.36 mm in the lateral view and 0.5 mm in the view from above for electrode 2. For both elements of electrode 9, the diameter was 0.58 mm in the lateral view and 0.63 mm viewed from above.

Our radiological measurements indicated a diameter of the cable of 0.5 mm, which was nearly the same as the published diameter (according to data sheet of MedEl company), suggesting that artefacts and diameters collected in this study are true. Otherwise, there should have been a significant difference between our CBCT-measured diameter of the cable and the real one.

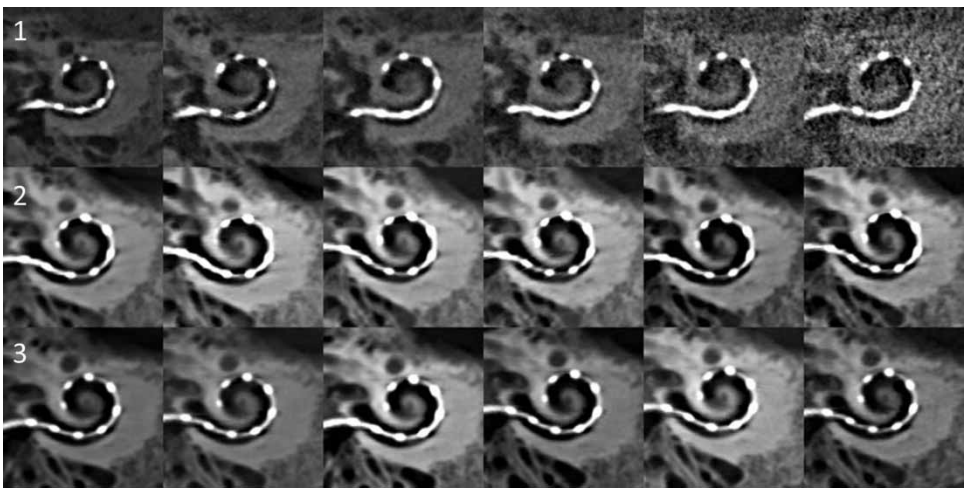

Figure 3 Differences of the imaging quality in association with the applied dosages are presented for all three groups (1, whole head; 2, temporal bone with whole implant; 3, temporal bone, electrode alone (without coil)).

Table 1 Overview of the measured diameters of the electrode (inclusive of artefact) (rows 1 and 4)

		Real		Whole head		Temporal bone with electrode and coil		Temporal bone with electrode alone	
	Electrode	View from above	Lateral view	View from above	Lateral view	View from above	Lateral view	View from above	Lateral view
Diameter (mm)	9	0.63	0.58	1.23*/**		1.43*		1.44**	
Proportion of artefact (%)	9			48.78	52.85	55.94	59.44	56.25	59.72
Mean proportion of artefact (%)	9			50.81*/**		57.69*		57.98**	
Diameter (mm)	2	0.50	0.36	0.97*/**		1.09*		1.08**	
Proportion of artefact (%)	2			48.45	62.89	54.13	66.97	53.70	66.67
Mean proportion of artefact (%)	2			55.67*/**		60.55*		60.19**	

The artefact rates in comparison to actual diameters are given for views from above and lateral views (rows 2 and 5). The mean artefact rates of the two values are given in rows 3 and 6. Highly significant differences ($P < 0.001$) are marked with * and **.

An overview of the following results and the statistical correlations is presented in Tables 1 and 2.

In group 1 (whole head), the mean diameter of electrode 9 inclusive of the artefact was 1.23 ± 0.03 mm. In comparison to the real diameter, this corresponded to an amplification ratio of 212% in the view from above and 195% in lateral view, compared with the true diameter, with a mean artefact rate of 50.81%. In group 2 (temporal bones with implant), the mean diameter was 1.43 ± 0.03 mm. This resulted in an artefact proportion of 57.69% and an amplification ratio of 247% for the view from above and 227% for the lateral view. In group 3 (temporal bone with the electrode alone), a mean diameter of 1.44 ± 0.03 mm was determined. This equated to an artefact proportion of 57.98% with an amplification ratio compared with the actual diameters of 248% in the view from above and 229% in lateral views. The mean diameter of the cochlea at the point of electrode 9 was 1.79 ± 0.11 mm. Therefore, results for electrode 9 inclusive of its radiological artefact were 68.71% of the cross-sectional cochlear diameter in group 1, 79.89% in group 2, and 80.45% in group 3.

For electrode 2, the mean diameter of the electrode in group 1 was 0.97 ± 0.05 mm. This was equivalent to an artefact proportion of 55.67%, with an amplification ratio of 270% for the view from above and of 194% for the lateral view. In group 2, the artefact proportion was 60.55% with a mean diameter of 1.09 ± 0.05 mm. The amplification ratio was 303% for the view from above 218% for the lateral view. An artefact proportion of 60.19% was recorded in group 3. The mean diameter was 1.08 ± 0.07 mm and the amplification ratio for the view from above was 300% and 216% for the lateral view. The diameter of the cochlea at the point of electrode 2 was 1.24 ± 0.04 mm. In consequence, the electrode inclusive of its artefact represented 78.23% of the cross-sectional cochlear diameter in group 1, 87.90% in group 2, and 87.10% in group 3.

The differences between the results of the whole head (group 1) and both groups of temporal bones (groups 2 and 3) were highly significant ($P < 0.001$) for the artefact proportions as well as for the proportion of electrode to cochlear diameters (Tables 1 and 2).

In detailed analysis, no significant influence of x-ray tube, x-ray current, or x-ray rotation angle could be determined. In particular, artefact proportions were completely independent of x-ray tube adjustments.

Discussion

Next to intraoperative electro-acoustical measurements, radiological imaging is the main technique for

Table 2 Overview of the measured diameters of the electrodes (inclusive of artefact) (rows 1 and 4) and the measured diameters of the corresponding cross-section of the turn of the cochlea (rows 2 and 5)

	Electrode	Whole head	Temporal bone with electrode and coil	Temporal bone with electrode alone
Diameter of the electrode (mm)	9	1.23 ± 0.03 */**	1.43 ± 0.03 *	1.44 ± 0.03 **
Diameter of the cochlea (mm)	9	1.78 ± 0.10	1.79 ± 0.11	1.79 ± 0.10
Relation electrode to cochlea (%)	9	68.71 */**	79.89 *	80.45 **
Diameter of the electrode (mm)	2	0.97 ± 0.05 */**	1.09 ± 0.05 *	1.08 ± 0.07 **
Diameter of the cochlea (mm)	2	1.24 ± 0.03	1.24 ± 0.04	1.23 ± 0.03
Relation electrode to cochlea (%)	2	78.23 */**	87.9 *	87.1 **

The resulting proportions of electrode to cochlear diameter are shown in rows 3 and 6. Highly significant differences ($P < 0.001$) are marked with * and **.

determining the correct intracochlear position of cochlear electrodes. However, which imaging technique is the most suitable remains under debate. Currently, CT is the gold standard and has allowed excellent visualization of the electrode in the basal part of the cochlea (Majdani *et al*., 2009; Trieger *et al*., 2011; Aschendorff *et al*., 2007). CBCT is a newer technique that provides imaging of thin bony structures with high accuracy in the anterior and lateral skull base (Güldner *et al*., 2011a; Bremke *et al*., 2010). Peltonen *et al*. (2009) demonstrated that CBCT could produce detailed, nearly artefact-free images of anatomical landmarks in the temporal bone as well as of the middle ear prosthesis. The potential of CBCT as a postoperative radiological tool after cochlear implantation was shown by Ruivo *et al*. (2009). The identification of the different intracochlear positions of the electrodes is possible by visualization with CBCT in isolated temporal bones (Aschendorff *et al*., 2004). In a comparison of radiological and histological images of cochlear electrodes in isolated temporal bones, Kurzweg *et al*. (2011) demonstrated safe evaluation and anatomical precision in the basal turn of the cochlea. Thus, to date, research on CBCT and CT imaging and artefacts of cochlear implants has been concentrated on isolated temporal bones. In a previous study of our group, artefact proportions of about 50% in visualization by CBCT were shown (Güldner *et al*., 2011b). The strength of this study was the focus on visualization of cochlear implants in whole human heads. In a previous retrospective analysis of patient data, it was found nearly impossible to obtain reliable evaluation of the intracochlear position of the electrodes in the medial and apical turns of the cochlea (Güldner *et al*., 2012).

As a continuation of these two previous studies, the aim of this study was to evaluate and compare the proportions of radiological artefacts of cochlear implants in CBCT images of the whole heads with those found in CBCT images of isolated temporal bones, and to look for any limitations in the use of isolated temporal bones in such imaging studies. The study included three complete human heads, into which were implanted MedEl flex soft electrodes. CBCT artefacts were examined at the basal and apical parts of the electrode array, and in whole head images a significant difference between radiological and real electrode diameters was found, with artefact proportions of 51% in basal and 56% in apical parts. Interestingly, in the images of temporal bones, both with and without implant receiver coils, significantly higher artefact proportions were determined in comparison to the whole head images (basal 58 and 59% and apical 61 and 60%). From our point of view, this is related to the physical background in which irradiation of metal substances results in imaging artefacts. The shape of an artefact depends on the magnitude of the incoming x-rays reaching the surface of the metal. In the case of the temporal bones, lower absorption of radiation by soft tissue results in greater surface radiation at the surface of the metal, and so to greater artefacts. In case of whole heads, there is a higher rate of absorption by surrounding soft tissue and bony structures, resulting in smaller metal artefacts.

In comparison to the corresponding cross-sectional diameter of the turn of the cochlea, the images of the electrodes, including radiological artefacts, occupy between 69 and 80% of the diameter of the cochlea in the basal part and between 78 and 88% in the apical part. Again, in the temporal bone images these proportions were significantly higher than the results in the whole head, which suggests that an absolutely safe evaluation of the intracochlear position of the electrodes, regarding its position in the scala tympani is still not possible. There was a trend for the images of the whole head to be more accurate than the isolated temporal bone images. The higher proportion of the electrode diameter to that of the cochlea in the apical part of the cochlea indicates that there is a progressive difficulty of safe evaluation in the thinner and more apical locations.

A limitation of this study is that the examinations were performed with only one CBCT device, and possibly different results might be determined with other devices. However, from the technical viewpoint, possible differences with other devices exist in the applied dosage and the post imaging procedures. In this study and one other, no correlation between the applied dosage and the rate of artefacts could be found (Güldner *et al*., 2011b). This is why we do not believe there are likely to be significant differences among different CBCT devices. Further studies focusing on artefacts with other CBCT devices, as well as in comparison with CT devices, are recommended and are already on-going.

In conclusion, because there is less soft-tissue absorption of radiation in isolated temporal bones, with a resulting higher level of stray radiation, there are significantly greater artefacts in images obtained from cochlear electrodes in isolated temporal bones than in images obtained from whole human heads. Therefore, studies with focus on imaging quality and artefacts from isolated temporal bones should be rated critically.

References

Aschendorff A., Kubalek R., Hochmuth A., Bink A., Kurtz C., Lohnstein P., *et al.* 2004. Imaging procedures in cochlear implant patients – evaluation of different radiological techniques. *Acta Otolaryngol Suppl*, 552: 46–49.

Aschendorff A., Kromeier J., Klenzner T., Laszig R. 2007. Quality control after insertion of the nucleus contour and contour advance electrode in adults. *Ear Hear*, 28: 75S–79S.

Bremke M., Leppek R., Werner J.A. 2010. Digital volume tomography in ENT medicine. *HNO*, Aug;58(8): 823–832.

Dalchow C., Weber A., Bien S., Yanagihara N., Werner J. 2006a. Value of digital volume tomography in patients with conductive hearing loss. *Eur Arch Otorhinolaryngol*, 263: 92–99.

Dalchow C.V., Weber A.L., Yanagihara N., Bien S., Werner J.A. 2006b. Digital volume tomography: radiologic examinations of the temporal bone. *Am J Roentgenol*, 186: 416–423.

Güldner C., Diogo I., Windfuhr J., Bien S., Teymoortash A., Werner J.A., *et al.* 2011a. Analysis of the fossa olfactoria using cone beam tomography (CBT). *Acta Otolaryngol*, 131: 72–78.

Güldner C., Wiegand S., Weiss R., Bien S., Sesterhenn A., Teymoortash A., *et al.* 2011b. Artifacts of the electrode in cochlea implantation and limits in analysis of deep insertion in cone beam tomography (CBT). *Eur Arch Otorhinolaryngol*, 2012 Mar;269(3): 767–772.

Güldner C., Weiss R., Eivazi B., Bien S., Werner J.A., Diogo I. 2012. Intracochlear electrode position: evaluation after deep insertion using cone beam computed tomography. *HNO*, Sep;60(9): 817–822.

Kolditz D., Struffert T., Kyriakou Y., Bozzato A., Dorfler A., Kalender W.A. 2011. Volume-of-interest imaging of the inner ear in a human temporal bone specimen using a robot-driven C-arm flat panel detector CT system. *AJNR Am J Neuroradiol*, 2012 Nov;33(10): E124–E128.

Kurzweg T., Dalchow C.V., Bremke M., Majdani O., Kureck I., Knecht R., *et al.* 2011. The value of digital volume tomography in assessing the position of cochlear implant arrays in temporal bone specimens. *Ear Hear*, 31: 413–419.

Majdani O., Thews K., Bartling S., Leinung M., Dalchow C., Labadie R., *et al.* 2009. Temporal bone imaging: comparison of flat panel volume CT and multisection CT. *Am J Neuroradiol*, 30: 1419–1424.

Peltonen L.I., Aarnisalo A.A., Kaser Y., Kortesniemi M.K., Robinson S., Suomalainen A., *et al.* 2009. Cone-beam computed tomography: a new method for imaging of the temporal bone. *Acta Radiol*, 50: 543–548.

Ruivo J., Mermuys K., Bacher K., Kuhweide R., Offeciers E., Casselman J.W. 2009. Cone beam computed tomography, a low-dose imaging technique in the postoperative assessment of cochlear implantation. *Otol Neurotol*, 30: 299–303.

Trieger A., Schulze A., Schneider M., Zahnert T., Murbe D. 2011. *In vivo* measurements of the insertion depth of cochlear implant arrays using flat-panel volume computed tomography. *Otol Neurotol*, 32: 152–157.